DOI: 10.13009/EUCASS2023-645
Aerospace Europe Conference 2023 – 10TH EUCASS – 9TH CEAS

Satellite Water Propulsion: Electrolyzer Development and Failure Mode Analysis

Alexandros Vikas†, Jérôme Hildebrandt*, and Stefanos Fasoulas*.*
** Institute of Space Systems*
Pfaffenwaldring 29, 70569 Stuttgart
vikasa@irs.uni-stuttgart.de – jhildebrandt@irs.uni-stuttgart.de – fasoulas@irs.uni-stuttgart.de
† Corresponding Author

Abstract
With the impending ban on hydrazine in the space sector, a great interest in green propulsion systems has developed. Therefore, the Institute of Space Systems of the University of Stuttgart is developing a water propulsion system that is scheduled to fly on the institute's ROMEO mission at the end of 2025. This work focuses on redesigning and improving the flight-capable electrolysis unit. To determine the cause of losses, impedance measurements are conducted on the static-water-fed electrolyzer. The data is used to improve the cell design by using porous media to increase water diffusion rates. A failure mode and effects analysis (FMEA) of water propulsion systems is conducted and applied to the design to improve system reliability.

1. Introduction and Motivation

The Institute of Space Systems (IRS) at the University of Stuttgart is developing a green electrolysis-based water propulsion system for satellites. One primary goal is to replace the commonly used hydrazine for higher thrust propulsion. Due to its extreme toxicity, using hydrazine is a risk for operators and the environment in case of an accident and might be banned in the EU soon. Using water instead, which is decomposed in orbit, increases fuel efficiency and drastically decreases the handling complexity and costs, making it attractive to smaller institutions. The water propulsion system in development at the IRS is one of the technology demonstrations on the institute's ROMEO mission, a small satellite with a planned launch date in 2025, where the water propulsion system shall be used to reach an elliptical medium earth orbit from a low earth orbit [1]. A prototype of this propulsion system has previously been successfully built and tested at IRS [2, 3]. This work aims to develop a novel 30 W, 50 bar electrolyzer with an integrated gas tank operating through the static-water-fed principle.

1.1 Motivation

Hydrazine-based chemical thrusters are the standard for satellite propulsion systems [4]. Even though the number of active satellites with electrical propulsion systems is steadily increasing [5], they are not generally a suitable replacement for chemical propulsion systems for every satellite mission, as they come with a high-power demand, which usually drives the satellite's electrical power system dimensions and consequently increases their dry mass. Furthermore, they have a much lower thrust level, which prolongs transfer maneuvers. Most LEO or MEO missions do not have a high Δv-demand, so their increased propellant efficiency is often not worth the drawbacks.

Today, most chemical thrusters are based on hydrazine, as this propellant offers simple and light systems with relatively high efficiency, either as monopropellant or bipropellant with NTO. Its imminent ban however, further encourages the development of green propulsion systems. Many of them are less toxic than hydrazine and could act as an alternative if the ban took effect. Nonetheless, they would not solve the other downsides, such as the immense costs involved due to the necessary safety measures, making it impossible to use for smaller institutions.

The strength of water electrolysis propulsion (WEP) is that it runs on inert water. Only in orbit the water is decomposed through electrolysis and gradually stored in small separate gas tanks for oxygen and hydrogen. After reaching a certain pressure level, a thrust maneuver can be performed by injecting both gases in the combustion chamber, where ignition is initiated by a catalyst. The fluid schematic for a WEP system is illustrated in Fig. 1.

DOI: 10.13009/EUCASS2023-645

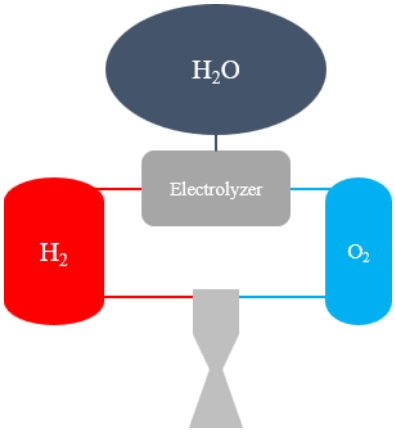

Figure 1: Fluid schematic of the water propulsion system

NASA has investigated water electrolysis propulsion since the 1960s [6]. In 1997, De Groot presented the first full-scale propulsion system for satellites using PEM electrolysis and the static water feed principle [7]. The first and, until today, only water electrolysis propulsion system in orbit was launched in 2021 on NASA's Pathfinder Technology Demonstrator and is called HYDROS® [8]. It delivers a nominal thrust of 1.2 N with 310 s specific impulse and is operated in the 5-25 W range according to Tethers Unlimited Inc. specifications [9].

One major drawback of the WEP systems electrolyzer previously developed at the IRS lies in severe current density drops at pressures above 15 bar, reducing its efficiency and gas production rates. In the course of this paper the cause of these losses is investigated through electrochemical impedance spectroscopy and used to redesign the electrolyzer's cells.

Additionally, a failure mode and effect analysis (FMEA) is conducted for the flight-capable system, and adequate redundancy and valve concepts are elaborated and integrated into the system design. Membrane ruptures in electrolyzers can lead to catastrophic failures, especially in the static water feed system, with cells directly connected to the gas tanks. Hydrogen diffusion through the membrane is an equally critical aspect to investigate. This paper also discusses the designed valve plan to mitigate the existing risks and minimize the risk for a loss of mission.

2. Electrolyzer principles

In-space electrolysis systems' major challenge is the production of dry hydrogen and oxygen in a microgravity environment. When the gases are intended as propellants, leftover water lowers the thruster's specific impulse and can lead to clogged propellant pipes or valves. Usually, ground-based electrolyzers use gravity for gas separation and utilize pumps to remove gases from the cell and provide new water to the system. The current state-of-the-art systems are the Oxygen Generation Assemblies (OGA) onboard the ISS in the European and US module [10, 11]. Both operate as alkaline electrolyzers and use rotary separators to separate hydrogen and undecomposed water. While the OGAs achieve high efficiencies, the complexity and weight of the peripheral systems are too high for small satellites. Additionally, using alkaline electrolytes places high requirements on seals and can cause damage to surrounding systems in the event of leakage.

With these challenges in mind, more attention has shifted towards solid polymer electrolysis (SPE) for its application in space [12]. Proton exchange membranes (PEM), which are sulfonated fluoropolymers, are used and act as the electrolyte. They are often referred to by the proprietary name Nafion®. At its Teflon®-like backbone, sulfonic-acid side chains are attached, enabling hydrogen proton conduction through the membrane. Water decomposition by electrolysis always follows the reaction shown in Eq. 1. To achieve the highest efficiency with PEM electrolyzers, the water is fed from the anode side, where it is decomposed into oxygen and hydrogen ions, as shown in Eq. 2. The hydrogen ions migrate to the cathode and are reduced to form hydrogen molecules shown in Eq. 3. As it is the case for all acid based electrolyzers.

$$H_2O \rightarrow H_2 + {}^1/_2\, O_2 \tag{1}$$

$$2\, H_2O \rightarrow O_2 + 4H^+ + 4e^- \tag{2}$$

DOI: 10.13009/EUCASS2023-645

$$2\,H^+ + 2e^- \rightarrow H_2 \tag{3}$$

For the reaction to take place sustainably under standard conditions (1013 hPa, 25 °C), the voltage applied in between the electrodes has to exceed the thermo neutral voltage of 1.48 V, following Eq. 4. With ΔH^0 describing the enthalpy of formation of water, F the Faraday constant, and z the number of electrons flowing for each molecule, in this case, 2. The voltage of 1.48 V does not account for additional losses inside the cell, like ohmic, polarization, and activation overpotentials. To keep them as low as possible, the contact between the electrodes and the membrane should be as high as possible. Additionally, catalysts are applied directly to the membrane. Together they form the so-called membrane electrode assembly (MEA) [13].

$$U_{th} = \frac{\Delta H^0}{zF} = 1.48\,V \tag{4}$$

When the water is supplied from the cathode side, oxygen is produced with low humidity. This comes at the cost of lower efficiencies since the evolution reactions, as stated in Eq. 2 and 3, still apply, and the hydrogen ions have to flow against the direction of the water.

By adding a membrane in front of the cathode, called water feed barrier (WFB), the water flow into the cell can be regulated to match the amount of water decomposed inside the cell since the concentration gradient across it drives the water diffusion through the membrane. Therefore, dry oxygen and hydrogen with low humidity can be produced. As this further increases the distance the water travels before reaching the cathode, the efficiency is decreased even further. The principle is depicted in Fig. 2. Another benefit of the static-water-fed concept is that the water pressure can be lower than the gas pressure inside the cell, thus making the need for pumps obsolete. Gas separators can be omitted as well, although desiccators might be needed if the operating conditions inside the cell cannot be kept in an optimal range to guarantee that the hydrogen stays below a required humidity level [7].

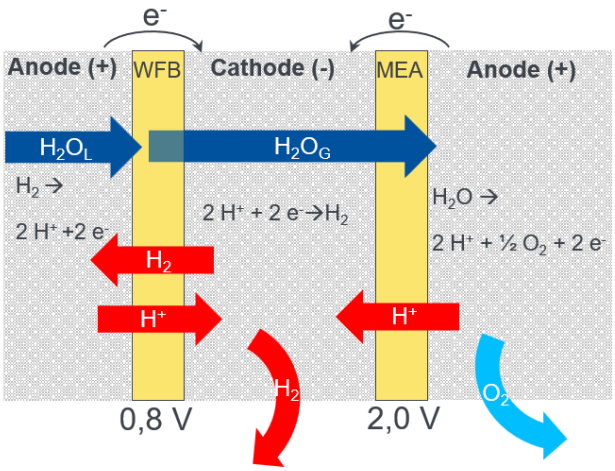

Figure 2: Working principle of the static-water-fed electrolyzer

The amount of gas produced at any given time can be described with Faraday's law shown in Eq. 5 with m the mass of the produced gas, M the molar weight for the species, and t the time in seconds. It can be seen that the gas production rate is solely dependent on the applied current. To shorten the mission duration, a high gas production rate is desirable and should therefore be aimed upon.

$$m = \frac{MIt}{zF} \tag{5}$$

When the water pressure is below the gas pressure inside the cell, hydrogen diffuses towards the side with water. An electrochemical hydrogen pump is implemented to keep the water compartment free of hydrogen and prevent the masking of the water feed barrier and consequently stopping the water flow. Applying a low voltage on the membrane pumps diffused hydrogen back to the electrolyzer's cathode. The voltage needed mainly depends on the pressure difference between the water and gas sides. It follows the Nernst equation shown in Eq. 6, with R the universal gas constant, p the pressure at the cathode and anode, and T the cell's temperature. It should be noted that

DOI: 10.13009/EUCASS2023-645

the Nernst voltage only accounts for the temperature and pressure difference. Additional losses occur, primarily kinetic losses at the electrode. Therefore, catalysts are used for the hydrogen pump, like in the cell.

$$U_{Nernst} = \frac{RT}{2F} \ln\left(\frac{p_{cat}}{p_{an}}\right) \quad (6)$$

To store and pressurize the gases, gas tanks can be directly attached to the cell and be sealed off. The hydrogen pump maintains the increase in pressure. Since gases are produced in a stochiometric ratio, the complete hydrogen compartment has to be double the size of the oxygen compartment to ensure both gases are stored at the same pressure.

In recent years anion exchange membrane (AEM) electrolysis has received increased attention, as a cheaper alternative to PEM [14]. AEMs are closely related to PEM membranes only that instead of hydrogen protos, OH^- - Ions are conducted, defining it as alkaline electrolysis. This allows the use of cheaper metals, that don't need to withstand the sour milieu, which limits one to titanium, and cheaper catalysts like nickel instead of platinum. The major downside of AEM electrolyzers lies in their considerably lower current density of 200-500 mA/cm^2 compared to 800–2500 mA/cm^2 achieved by PEM.

For alkaline electrolysis Eq. 1 is still valid but the anode and cathode reaction change to the equation shown in Eq. 7 and 8 respectively.

$$2\ OH^- \rightarrow \frac{1}{2} O_2 + H_2O + 2e^- \quad (7)$$

$$2\ H_2O + 2e^- \rightarrow H_2 + 2OH^- \quad (8)$$

It should be pointed out, that an AEM switches the flow of the ions, which then go from the cathode to the anode.

3. Experimental

3.1 Previous Design

The electrolyzer used as a benchmark was developed by Harmansa [3] and was intended for operation at 20 W with a gas pressure of up to 50 bar. It consists of two fully redundant cells with an active area of 50 cm^2 each. The membranes for the water feed barrier as well as the MEA, are Nafion 115 with a platinum catalyst loading of 1 mg/cm^2 platinum on the cathode and 2 mg/cm^2 of iridium on the anode side. The bipolar plates are grid-structured titanium plates with a porosity of 50 %, allowing for large gaps where the water vapor can pass through to the MEA. To increase the contact with the MEA, a carbon cloth gas diffusion layer is inserted on the cathode side, and titanium felt on the anode. The temperature is regulated through a heating strip attached to the outside of the electrolyzer.

Harmansa conducted the characterization of the cell, and are depicted in Fig. 3. The measurements were stopped after reaching over 20 bar of H_2 pressure because of sealing issues resulting in ongoing leakage of both gases. It can be noted that the current density decreases rapidly with increasing pressure, which lowers the cell's efficiency and gas production rate. To further investigate this phenomenon, impedance spectroscopy measurements are conducted to locate the leading cause of losses.

DOI: 10.13009/EUCASS2023-645

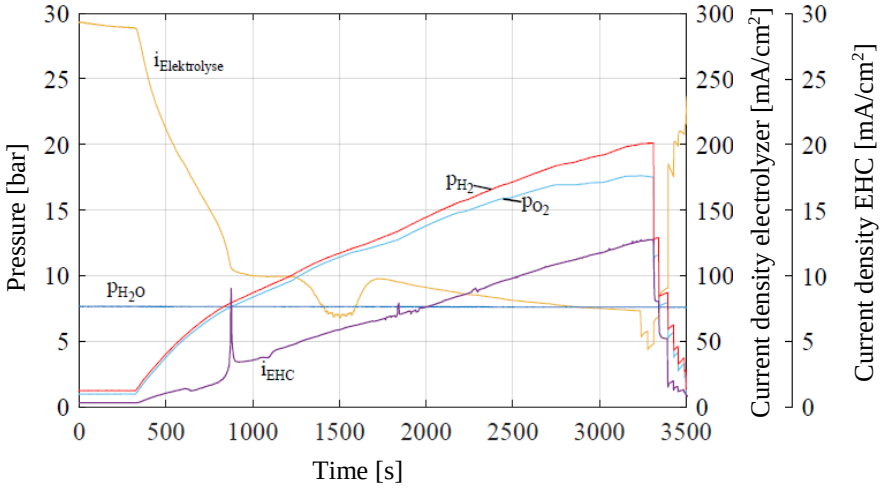

Figure 3: Pressure and current density plot over time of the electrolyzer [3]

3.2 Impedance Spectroscopy Measurements

Electrochemical impedance spectroscopy (EIS) measurements are conducted using a Zahner IM6 frequency response analyzer and a Zahner PP241 potentiostat in a two-electrode set-up, where the anode is connected to the working electrode and the cathode acts as the reference electrode. The spectra are measured potentiostatically between 10 kHz and 0.1 Hz with 10 points per decade. For the measurement, an AC voltage disturbance of 50 mV is applied on top of the DC operation voltage, which is kept at 2.0 V. The electrolyzer's operating temperature is kept between 70 °C and 72 °C. The water is supplied at ambient pressure to the water feed barrier, and the gas pressure inside the cell is kept constant through needle valves. To investigate the reasons for the ongoing decrease in current density, the measurements were performed at different gas pressure levels of 1, 2.5, 5.0, and 8.5 bar.

The data is fit to an equivalent circuit depicted in Fig. 4. It was selected with the approach most common for PEM electrolyzers in mind, which is to have three Voigt elements (capacitor or CPE and resistor in parallel) in series [15, 16, 17]. The first Voigt element (R_1/CPE_1) represents the cathode and faster hydrogen evolution reaction (HER). With a higher time constant, it can be found at higher frequencies and lower resistance and capacitance values. The second Voigt element depicts (R_2/CPE_2) the much slower oxygen evolution reaction (OER), taking place at the anode with a lower time constant. Instead of a third Voigt element, a Nernst diffusion (ND_2) is implemented. It reduces the number of elements that need to be fitted, and we already expect a high diffusion resistance due to the limited water supply, which will mainly show itself at the anode. Constant phase elements (CPE) are used as they better depict the reality of an imperfect electrode surface. They can interact with Warburg impedances like the Nernst diffusion. Therefore, particular attention has to be paid to their fitting results, especially the α value, which describes the deviation from an ideal capacitor and should stay in a range of 0.5 to 1 [18]. An inductance (L_0) and a resistor (R_0) are added to the two Voigt elements to depict the inductive and ohmic behavior of all conductors inside the cell.

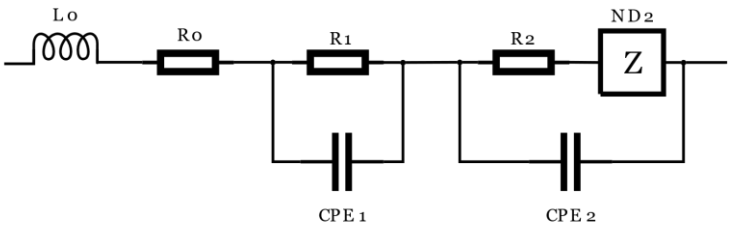

Figure 4: Equivalent circuit for impedance data fit

The values for the equivalent circuit are fitted to the measurements with the Zahner Analysis software using a complex non-linear regression least-squares fitting algorithm. The fitting is finished when the absolute error between the measured and modeled values falls below 0.1% or the relative improvement between two iteration steps is below 10^{-7} [18].

DOI: 10.13009/EUCASS2023-645

4. Results

4.1 Impedance Data

Fig. 5 depicts the results of the EIS measurements in a Bode and Nyquist plot with their respective fitted curves. What sticks out is the strongly pronounced diffusion arc at low frequencies, visible in the Nyquist plot at the higher end of the real resistance. As the electrolyzer is operated in a diffusion-limited state, this behavior is expected. Additionally, we can make out a drift of the whole curve towards higher real resistances, as well as an increase of the second arc with increasing pressures. A slight increase of the firsts arc diameter, depicting the cathode and HER, can be noted as well.

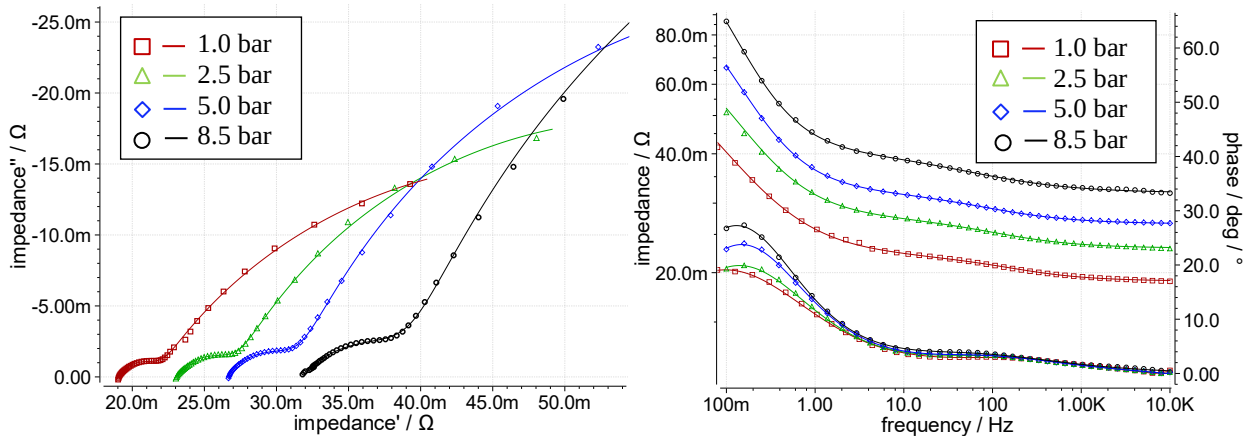

Figure 5: Nyquist and Bode plot of EIS measurements at 1.0, 2.5, 5.0, and 8.5 bar.

In Tab. 1, the values for the equivalent circuit fit are given, as well as the voltage and current for each measurement and the overall error of the fit. The ohmic resistance R_0 is steadily increasing with rising pressure. This behavior is also seen in the plots as the overall drift towards higher resistance. As R_0 depicts only resistances of a purely ohmic nature, we can assume that the increase results from a decrease in contact between the current collector plates and the electrodes due to physical separation.

Table 1: Electrolyzer values at pressures from 1.0 to 8.5 bar and values for fitted equivalent circuit components

Pressure [bar]		**1.0**	**2.5**	**5.0**	**8.5**
Current [A]		17.86	13.95	11.56	9.04
L_0 [nH]		4.41	3.65	3.45	0.75
R_0 [mΩ]		19.0	23.1	26.6	31.8
R_1 [mΩ]		2.6	4.0	5.1	7.9
CPE_1	C_{eq} [mF]	215	178	155	110
	α	0.71	0.67	0.65	0.58
R_2 [mΩ]		2.9	5.6	19.8	25.4
CPE_2	C_{eq} [F]	1.74	2.57	3.61	3.58
	α	0.62	0.70	0.77	0.80
ND_2 [mΩ/s$^{1/2}$]		98	116	289	290
Overall Err.		0.76%	0.85%	0.43%	0.61%

R1 shows progressively higher values as well, showing a slight increase in cathode resistance. At the same time, the time constant for the HER, inversely proportional to the product of capacitance and resistance, decreases slightly, suggesting a slightly slower creation of hydrogen.

DOI: 10.13009/EUCASS2023-645

The most pronounced differences can be seen in R_2, CPE_2, and the Nernst diffusion. With increasing pressure, the resistance strongly increases, and with it, the time constant of the OER decreases to a greater extent than the time constant at the cathode.

The decreasing inductance can be traced back to the decreasing current due to the increase in resistance. A lower current results in weaker magnetic fields.

Overall, two significant effects can be noted with increasing pressure. The first is the steady increase in ohmic resistance from the physical separation of the plates leading to an increase in contact resistance. The second is a continuous drying of the anode, resulting in a slower OER and lowering the efficiency.

4.2 New Cell Design

Following the results from the EIS measurements, a new iteration of electrolyzer cells is designed.

For the active area of the cell, 45 cm^2 has been selected. That allows for an operation at 2 V and 350 mA/cm^2 when 30 W is provided. The overall footprint of the cell was kept within 10 x 10 cm to allow for the use in 1 U of a satellite.

One cell consists of three plates, with each containing the volume for the three fluids, water, hydrogen, and oxygen. In between the plates the membranes are compressed. An explosion view of one cell and the top view of the hydrogen cell is depicted in Fig. 6. All plates follow the same layout, with a circular active area in the middle, containing the fluid volume and an octagonal border surrounding it, containing a wide flat seal and fluid channels. The threw-holes for the screws are placed in the border as well. For the moment three flat seal materials stand for selection, which are a fluoroelastomer, Polyolefin, or a silicon coated PET. Which material offers the best sealing capabilities and cell compression is still part of studies.

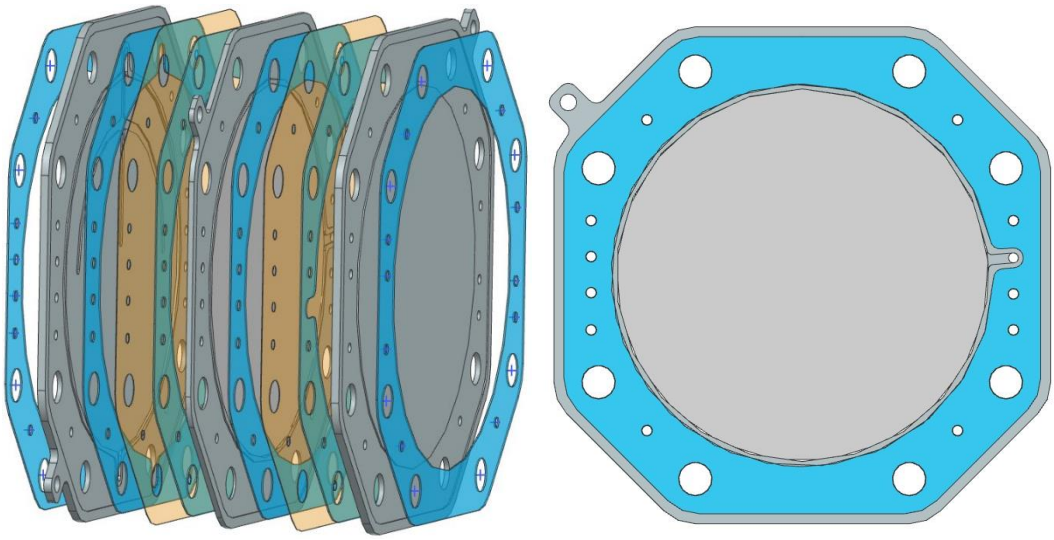

a) b)

Figure 6: a) Explosion view of one cell. b) Top view of the H_2 plate with inlaid flat seal.

The oxygen and water plate are closed on one side and the cell are is formed by a circular cavity. The created volume is then filled with titanium fiber felt or porous titanium frit of constant porosity to allow free fluid movement, high electrical contact with the membrane, and variate the cells compression. The active area of the hydrogen plate is formed by a porous titanium frit welded in place creating two empty volumes above and below it. These volumes are as well filled with a fiber felt or porous titanium frit. To match the stoichiometric amount of produced gases, the hydrogen cell's volume has double the oxygen cell's size. An adapted gas tank volume can compensate for a different cell design but requires all cells to be connected at the cost of redundancy. To avoid short circuits with the next cell and the surrounding, the bottom of the water and oxygen plate are coated with PTFE.

DOI: 10.13009/EUCASS2023-645

As water diffuses through the WFB in molecular form, it is initially present in a gaseous state. The operation temperature inside the cell is not intended to exceed 80°C. Therefore, water should condensate, especially at higher pressures and when the cell is not decomposing water at a high enough rate. This assumption is yet to be proven, and the aggregate state inside a static water-fed electrolyzer's cell hasn't been investigated yet.

If liquid water is present, capillary forces can be made use of to improve the water supply of the MEA and reduce the diffusion resistance at higher pressures. Following Eq. 9 this can be achieved by reducing the porosity and pore size towards the MEA inside the hydrogen plate [19]. With p_c the capillary pressure, σ the surface tension, θ the contact angle and r the pore radius. In the new cell design, a shrinking of the pore radius is realized in three steps, by filling the cavity in front of the welded titanium frit with an additional frit or fiber felt of greater pore size and behind with one of smaller pore size.

$$p_c = \frac{2\sigma \cos\theta}{r} \tag{9}$$

As shown in Fig. 2 the water has to travel a long way through the cell, crossing two membranes before it gets decomposed. At the same time, the water flow is impeded by H^+ ions traveling back to the cathode. Switching out the PEM MEA with an AEM would shorten the way the water has to travel, and match it with the flow of ions, which could lead to lower diffusion resistances. While AEM is known for lower current densities, the already achieved values still outperform the ones reached by static-water-fed electrolysis. As they are build up in the same manner, interchanging them in the electrolyzer should be feasible with minor adaptations.

4.3 Failure Mode and Effect Analysis

The primary fluid schematic, as depicted in Fig. 1, shows that all present media (water, hydrogen, and oxygen) unite in the electrolyzer and are only separated by the two membranes of the WFB and MEA. Under nominal operation, this does not pose any threat, but a critical condition can occur when the membranes do not operate as intended.

The far more threatening failure comes from the MEA. Without it, both gas tanks are connected, and a stochiometric gas mixture of oxygen and hydrogen is present. With the catalyst on the electrodes, an ignition can quickly occur. Apart from a membrane perforation, the gases can mix by diffusion through the membrane due to the large partial pressure difference, especially when the electrolyzer reaches higher pressures, which is the case during coasting phases, where the gas tanks are filled but engine ignition cannot be performed yet. To avoid an ignition inside the electrolyzer or the gas tanks, the amount of hydrogen in oxygen and vice versa should be kept below 4 mol% at any instance [20].

Bessarabov [21] elaborates that during nominal operation, cross-diffusion presents no critical issue for PEM electrolysis but becomes relevant at higher pressures (> 10 bar) and low current densities. While both gases are prone to diffusion through the PEM, hydrogen diffusion is the defining case. For one, hydrogen's permeability can be assumed to be roughly double that of oxygen. Second, the molar amount of stored oxygen in the system is always half the amount of hydrogen. Thus, a critical mol% of hydrogen in oxygen is reached earlier. At the same time, as long as the thermo-neutral voltage is applied, only electron-producing reactions can take place at the anode and electron-consuming reactions at the cathode. That means hydrogen crossing towards the anode is more likely to dissociate into protons and be pumped back than to react with oxygen. The oxygen reduction reaction can still occur at the cathode side, though it only occurs in equilibrium with hydrogen oxidation reactions at the anode, which is highly unlikely.

According to Bessarabov [21] it can be observed that at high pressures, hydrogen crossing over to the anode simply exits the anode with the produced oxygen. This links the pressure achievable inside the electrolyzer to a current density described in Eq. 10 with p_{H2} the pressure in bar, L_B the membrane thickness in m, k_{H2} the diffusion coefficient for hydrogen through Nafion defined in Eq. 11 [22], $x_{H2,Crit}$ the critical mol% of hydrogen in oxygen at the given pressure and i the needed current density in A/cm².

$$p_{H2} \leq L_B \left\{ \frac{1}{4Fk_{H_2}} \left(\frac{x_{H2,Crit}}{1-x_{H2,Crit}} \right) \right\} i \tag{10}$$

$$k_{H2} = 6.6 \times 10^{-8} \exp\left(-\frac{21\,030\ J\,mol^{-1}}{RT} \right) \tag{11}$$

DOI: 10.13009/EUCASS2023-645

The targeted 50 bar leaves us with a needed current density of 0.85 A/cm^2 for Nafion 117 and 1.20 A/cm2 for Nafion 115. These values have to this day not been reached by static-water-feed electrolyzers. Additionally, the ongoing current density drop with increasing pressure shown in Fig. 3 does not allow for pressures higher than 10 bar, without reaching critical gas mixtures for the current prototype. At the same time, it should be noted that these numbers have only been validated for liquid-fed electrolyzers and assume a thoroughly water-saturated PEM membrane. The cross-diffusion can be significantly lower in a dryer state and has yet to be fully investigated.

When the electrolysis unit is switched off, and the gases are stored under pressure, diffusion across the membrane still takes place. To prevent the formation of an explosive mixture, a voltage has to be constantly applied of at least 0.06 V according to Eq. 6, effectively creating a second hydrogen pump. The resulting current density must match the amount of hydrogen diffusing to the anode and is calculated with Eq. 12 derived from Eq. 10. For Nafion 117 and 50 bar of gas pressure 0.02 A/cm^2 are needed.

$$i_{H2,pump} = \frac{2Fk_{H2}}{L_B} p_{H2} \tag{12}$$

In case of a lack of applied voltage, the time it takes for an explosive mixture to be present depends on the volume of the gas compartment and the membrane thickness.

Constantly applying a voltage on the MEA can be a challenging task for the satellite's power system, especially if the satellite enters a power-saving safe mode. Additional batteries or capacitors might have to be foreseen to prevent safety-critical gas mixtures. What still cannot be accounted for are membrane ruptures or pin holes that can form through mechanical stress or local heat increase. These holes create short circuits and make the cell inoperable. The produced gases stored in the gas tanks have to be prevented from mixing, which creates the need for some sort of valve between the gas tanks and the cell.

The second critical condition can occur at the water feed barrier. For one, hydrogen constantly diffuses towards the water tank when no voltage is applied. Therefore, a permanent voltage supply has to be foreseen at the WFB as well. Additionally, when the cell is switched off, water will keep on diffusing inside the cell until the concentration gradient across the membrane is low enough. When the cell is switched back on, this can lead to produced gasses with humidity reaching 100%.

In case of a WFB membrane rupture, water can pass unhindered through the cell to the gas tanks as long as the pressure inside the water tank is higher. This is especially the case at begin of life (BOL) when the water tank is still fully pressurized. One way to avoid this failure is to implement latching valves before the cells.

Apart from the membrane, off-nominal temperatures can also lead to system failures. With water as the primary present fluid, temperatures must be kept between 0°C and 100°C. Going below the freezing point can damage the membranes and all structural components, like tanks and electrolyzer plates. Above the boiling point, the pressure on the water side increases, reaching values outside the intended operational region. Additionally, inside the electrolyzer, the membranes can dry out, lowering the cell's efficiency, although not permanently. The latter must be further investigated, especially its implications for static-water-fed electrolysis.

Apart from fluid-related failures, electrical failures can occur. The most severe one is a short circuit, mainly through the perforation of the membranes. Over-current protections have to be foreseen to avoid further damage to the electrolyzer and electrical circuit.

4.4 New Electrolysis Unit

Following the results of the FMEA, a fluid circuit for the electrolysis and gas tank unit has been designed. It is depicted in Fig. 7. Each cell is foreseen three times in a power-limited, fully redundant manner. That means if the current density of 350 A/cm^2 is reached at any instance, the provided 30 W of power can be fully used for gas production. If the electrolyzer should still show a drop in current density with increasing gas pressure, two or three cells can be operated simultaneously, effectively increasing the cell area and compensating for the lower current density. Although, this comes at the cost of redundancy.

DOI: 10.13009/EUCASS2023-645

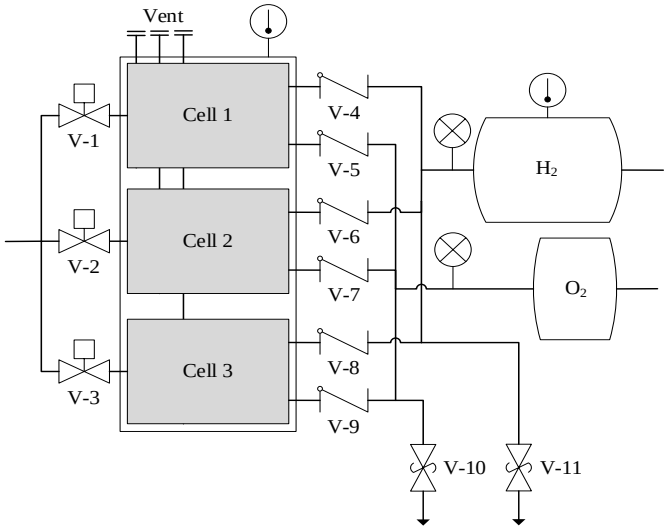

Figure 7: Valve circuit of the electrolyzer-gas-tank-unit [23]

On its way from the water tank, the water splits up into three separate channels with a latch valve on each (V-1 through V-3). The latch valve allows for the water flow to be stopped when the cell is not operated, limiting the diffusion into the cell and protecting the gas tank and cell from flooding in case of a membrane rupture. An alternative is to replace the latch valves with check valves. The alternative design would save 460 g on the overall unit, which comes in at 2.3 kg. Using check valves would require the gas pressure to always be above the water pressure in order to hinder flooding of the cell and gas tank. This limits the thrust duration at every maneuver, especially at BOL, and increases the time till the final orbit can be reached. In order to allow the cells to vent during the initial filling with water, vent lines are foreseen, which are sealed off after the filling process.

After every cell, check valves are implemented on the oxygen and hydrogen side (V-4 through V-9). They hinder an exchange with the gases in the tanks and the cell, ensuring that in the event of a membrane rupture or uncontrolled cross-diffusion, the amount of mixed gases is limited to only the amount inside the affected cell.

Relive valves can be foreseen at the gas tanks (V-10 and V-11), but where deemed unnecessary for the flight model. In the case that unwanted high pressures are reached, the gases can be released through the thruster valves, without causing an ignition. An uncontrolled gas production of the electrolyzer was also seen as unlikely as it can be switched of by its own power system, or by the satellites power distribution unit.

All three cells are arranged in a stack in alternating order. In that way, the oxygen and water plates of the two cells face each other. This configuration reduces the voltage and pressure difference between two neighboring cells.

The gas tanks are designed as one unit and integrated on top of the electrolyzer, doubling as the end plate. This reduces weight, as the end plate can be designed thinner since it sees only minor pressure difference between both sides during nominal operation. In case of a cell failure, the tank pressure has to be absorbed but in support of the whole electrolyzer. The gas tank size is chosen in a way that it takes two orbits (180 min) to fill with a 15 A operational current.

The second end plate doubles as a valve block, containing all valves for electrolyzer operation. Both plates are designed to be 3D printed with titanium.
The design also allows for additional cells without any needed changes, although without redundancy. Each cell can be copied multiple times and stacked upon each other at any amount desired. In that case, the system keeps its three redundant strings but can be operated at higher power levels. The current thereby stays the same for each string, and the needed voltage is a multiple of the operation voltage of a single cell. What thermal implications that has, has yet to be investigated.

The assembled three-cell unit can be seen in Fig. 7. On top of the gas tank, a frame is foreseen as an MLI bracket. The unit weighs 2.33 kg with latching valves and a 400 ml hydrogen and 200 ml oxygen tank. With the holding bracket it fits in a 200 x 140 x 120 mm box.

DOI: 10.13009/EUCASS2023-645

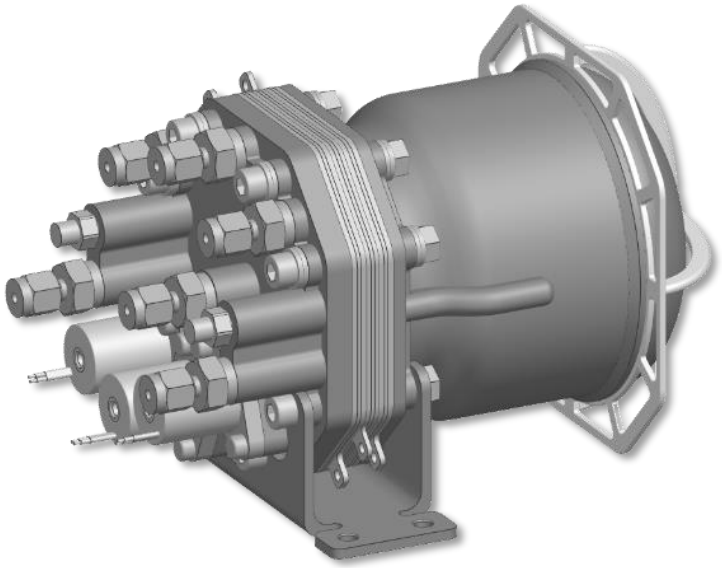

Figure 8: Assembly of the electrolyzer-gas-tank-unit with latch valves [23]

5. Summary and Outlook

With water electrolysis propulsion, an environmentally friendly alternative to hydrazine is available, which is also suitable for smaller institutions. The WEP electrolyzer intended to fly on the ROMEO mission still shows a notable efficiency decrease when operated at higher pressures, which would increase the transfer duration. The reasons for the observed current density drop were determined through electrochemical impedance spectroscopy and used to improve the next generation of the electrolysis unit. An FMEA was additionally conducted, and the results were applied to the new system design to mitigate possible failures and prevent a loss of mission.

Once built, the new electrolyzer unit will be investigated regarding its characteristics, gas humidity, and gas crossover. The analysis will be performed by varying the cell compression, membrane thickness, and the electrolyzer's orientation to estimate the effects of micro-gravitation. More in-depth EIS measurements will be conducted as well, applying the elaborated equivalent circuit for a better comparison to the previous generation.

Parallel to the electrolyzer unit, a semi-autonomous power system is being developed to monitor and operate the electrolyzer once in space. When both systems are operative, the FMEA will be conducted further to account for failures exceeding the cell.

Finally, a deeper look will be taken in anion exchange membranes as an alternative to PEM for static water feed electrolysis by replacing the MEA with an AEM.

DOI: 10.13009/EUCASS2023-645

References

[1] Loefler, T. et al. 2021. Research and Observation in Medium Earth Orbit (ROMEO) with a cost effective micro satellite platform. 72nd International Astronautical Congress (IAC), Dubai, 2021

[2] Harmansa, N. et al. 2019. Hybrid Electric Propulsion System based on Water Electrolysis. 36th IEPC, Vienna.

[3] Harmansa, N. 2020. Entwicklung und Charakterisierung eines Satellitenantriebssystems basierend auf Wasserelektrolyse. Dissertation University of Stuttgart

[4] European Commission: Making satellites safer: the search for new propellants. [accessed 2023-06-05]

[5] Lev, D. et al. 2017. The Technological and Commercial Expansion of Electric Propulsion in the Past 24 Years. 35th IEPC, Atlanta, USA.

[6] Rollbuhler, R. J. 1969. Experimental performance of a water-electrolysis rocket (No. NASA-TM-X-1737)#

[7] De Groot, W., Arrington, L., McElroy, J., Mitlitsky, F., Weisberg, A., Carter, II, P., ... & Reed, B. 1997. Electrolysis propulsion for spacecraft applications. In 33rd Joint Propulsion Conference and Exhibit p. 2948

[8] Marmie, John, et al. 2017. NASA's Pathfinder Technology Demonstrator.

[9] Tethers Unlimited Inc.: Propulsion System. (Accessed 2023-06-04) https://www.tethers.com/propulsion-system/

[10] Erickson, R. J., Howe, J., Kulp, G. W., & Van Keuren, S. P. 2008. International space station united states orbital segment oxygen generation system on-orbit operational experience. SAE International Journal of Aerospace, 1(2008-01-1962), 15-24.

[11] Witt, J., Hovland, S., Laurini, D., Matthias, C., Boettcher, F., Bevilacqua, T., & Redondo, C. 2020. On-orbit Testing of the Advanced Closed Loop System ACLS. 2020 International Conference on Environmental Systems.

[12] Sakurai, M., Sone, Y., Nishida, T., Matsushima, H., & Fukunaka, Y. 2013. Fundamental study of water electrolysis for life support system in space. Electrochimica Acta, 100, 350-357.

[13] Kurzweil, P., & Dietlmeier, O. K. 2016. Elektrochemische Speicher: Superkondensatoren, Batterien, Elektrolyse-Wasserstoff, Rechtliche Grundlagen. Springer-Verlag.

[14] Vincent, Immanuel; Bessarabov, Dmitri. Low cost hydrogen production by anion exchange membrane electrolysis: A review. Renewable and Sustainable Energy Reviews. 2018, 81. Jg., S. 1690-1704.

[15] Garcia-Navarro, Julio Cesar; Schulze, Mathias; Friedrich, Kaspar Andreas. , 2019 Measuring and modeling mass transport losses in proton exchange membrane water electrolyzers using electrochemical impedance spectroscopy. Journal of Power Sources, 431. Jg., S. 189-204.

[16] Frensch, Steffen Henrik, et al. 2018. Model-supported characterization of a PEM water electrolysis cell for the effect of compression. Electrochimica Acta, 263. Jg., S. 228-236.

[17] Siracusano, Stefania, et al. 2018. Electrochemical impedance spectroscopy as a diagnostic tool in polymer electrolyte membrane electrolysis. Materials , 11. Jg., Nr. 8, S. 1368.

[18] Zahner Analysis manual. (Accessed 2023-05-17) https://doc.zahner.de/manuals/zahner_analysis.pdf

[19] Fanchi, John R.. 2005. Principles of applied reservoir simulation. Elsevier. p. 32

[20] SCHRÖDER, Volkmar, et al. 2003. Explosionsgrenzen von Wasserstoff/Sauerstoff-Gemischen bei Drücken bis 200 bar. Chemie Ingenieur Technik.

[21] Bessarabov, Dmitri, et al. (Hg.). 2016. PEM electrolysis for hydrogen production: principles and applications. CRC press. pp. 253

[22] Kocha, Shyam S.; Deliang Yang, J.; Yi, Jung S. 2006. Characterization of gas crossover and its implications in PEM fuel cells. AIChE Journal, 52. Jg., Nr. 5, pp. 1916-1925.

[23] Wanke, David. 2023, Development of a compact gas tank and valve unit for a water electrolysis propulsion system